

Suppression of Catastrophic Motion and Horseshoes Chaos on a Mechanical Structure using Opto-Electromechanicals Devices

Daniel Junior Lissan 1er¹, Sanda Abbo Oumarou² and B.R. Nana Nbandjo^{*,3}

¹Laboratory of Energy Carnot, Department of Physics, Faculty of Science, University of Bangui, B.P. 1450 Bangui, Central African Republic, *Laboratory of Modelling and Simulation in Engineering, Biomimetics and Prototypes, Faculty of Science, University of Yaounde I, P.O. Box 812, Yaounde, Cameroon,

³Physics department, Faculty of Sciences, University of Bertoua, B.P. 416, Bertoua, Cameroon.

ABSTRACT We investigate in this paper the dynamic performance of an opto-electromechanicals control technics on a structure modelled by beam with degenerated ϕ^6 potential. The mathematical model of the structure under control has been derived. The dynamics response are explored using harmonic balance methods. The ability to dissipate the undesired vibrations of a these structures to an acceptable level is theoretically examined by derived the condition of escape from the potential well as well as the criteria for the occurrence of horseshoes chaos on the physical system. The effects of the appropriate control parameter leading to optimal control is explored. It appear globally that opto-electromechanical device is a good candidate of horseshoes chaos suppression on mechanical structures.

KEYWORDS

Escape boundary
Opto-electromechanical control
Basin of attraction
Horseshoes chaos

INTRODUCTION

In recent years, significant research has focused on controlling vibrations in structures across various domains of fundamental and applied sciences. The primary objectives in this field are to minimize vibration amplitudes, suppress chaotic behavior, and prevent escape from potential wells. These efforts have numerous applications in structural mechanics (Aida *et al.* 1995; Okada *et al.* 1995; Hackl *et al.* 1993; Cheng *et al.* 1993). Under the influence of the external excitations, the mechanical structures enter in resonance and sometimes become very unstable. A strategy of controls of vibrations, quite elaborate makes it possible to ensure the protection of the structures against these sources of instabilities (Sonfack 2011; Nana Nbandjo 2004). During these last years, much of scientific research tasks were realized, mainly on the active structural vibrations controlled by traditional electromechanical transducers such as the piezoelectric actuators, electrostrictives, and magnetostrictives (Metsebo *et al.* 2024; Wang *et al.* 2001; Tzou and Anderson 1992; Ngatcha *et al.* 2024; Shih 2000).

These traditional actuators which, formerly, were connected to the cables for the transmission of the signals of control are replaced by the actuators opto-electromechanicals without wire. Even if the presence of an external electromagnetic field in the environment creates many electromagnetic interferences, its impact is minimized by the opto-electromechanical actuators without wire. Recently, the researchers developed a strategy of control which uses a photostrictif material to produce a constraint on the surface of a structure (Fukuda *et al.* 1993; Uchino 1996). Liu *et al.* (Liu and Tzou 1998b) studied the couplings of the photo constriction, the photo deformation, pyroelectricity, thermoelasticity, photostrictive opto-piezo-thermoelasticity and the release planar opto-electromechanical two-dimensional. Recently Shih *et al.* (Shih and Tzou 2000) developed a framework of opto-electromechanicals control for application on vibration reduction of mechanical structures and presented a model of photostrictive actuators distributed in one and two dimensions.

After the mathematical modelling of the structure under opto-electromechanical control, we explore the dynamics of the system using harmonic balance method and then derive the maximum energy of the system and then the escape boundary condition. This allows us to derive in the space parameters of the system the escape condition. In other to predict the appearance of horseshoes chaos, we use the Melnikov theory (Moon 1992; Nana Nbandjo *et al.* 2003; Pinto and Goncalves 2002; Nana Nbandjo and Wofo 2007),

Manuscript received: 11 July 2024,

Revised: 30 September 2024,

Accepted: 19 October 2024.

¹djlissan1er@gmail.com

²oumarabo5@yahoo.fr

³nananbandjo@yahoo.com (Corresponding author)

which permits to derive the analytical criteria for the occurrence of transverse intersections on Homoclinic and Heteroclinic orbits for the case of unbounded double well potential. For each case, analysis has been done to derive a good parameter leading to optimal control. We end by the conclusion.

MODELING AND GENERAL MATHEMATICAL FORMALISM

An opto-electromechanic actuator also known as photostrictive actuator, can be defined as a building able to produce, with the help of a suitable illumination, a considerable mechanical action (deformation, force, moment) (Carlioz 2009). The operation of the opto-electromechanic actuators rests basically on two physical phenomena which are the photovoltaic effect and the piezoelectric effect. However other phenomena such as the pyroelectric and the thermoelastic effects can be taken into account (Liu and Tzou 1998a).

Modeling of an opto-electromechanic actuator

Consider a rectangular opto-electromechanic actuator of bimorph type having a length a_0 , one width b_0 , and a thickness h_0 , as indicated in Figure 1. Various physical phenomena whose appear in this actuator is described in (Shih et al. 2005).

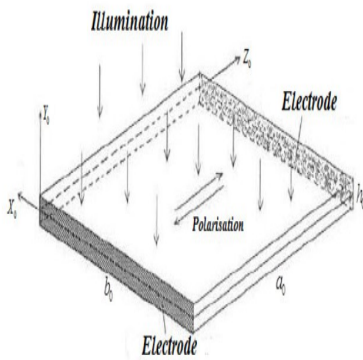


Figure 1 Opto-electromechanic Actuator under luminous irradiation (Carlioz 2009).

The deformation of an opto-electromechanic actuator comes from the superposition of the principal following effects: The combination of the photovoltaic and piezoelectric effects. This allows to derive equation 1 (see ref Carlioz (2009))

$$[S_{0-e}(t_j) = d_{33} \cdot E_{ph}(t_j) = d_{33} \cdot \left(\begin{array}{l} [E_s - E_{ph}(t_{j-1})] \alpha_0 I(t_j) \Delta t e^{-\alpha_0 I(t_j) \Delta t} \\ + E_{ph}(t_{j-1}) - E_{ph}(t_{j-1}) \beta_0 \Delta t e^{-\beta_0 \Delta t} \end{array} \right) \quad (1)$$

where $S, d_{33}, E_{ph}, E_s, I, \alpha_0$ and β_0 are respectively:

- S : Deformation,
- d_{33} : The piezoelectric constant,
- E_{ph} : The electric field induced by the photovoltaic effect,
- E_s : The photovoltaic saturating field,
- I : Intensity of illumination,
- α_0 : The constant of the actuator opto-electromechanics,
- β_0 : The constant of pressure loss.

The servo-control (Tzou and Chou 1996) of an opto-electro mechanical actuator uses two signals at the entry: the standard

signal which is reproduce by the actuator and the control signal useful for the activation of this last. A sensor measures the tension induced by the actuator or its deformation, the drifting signal of this measurement is introduced then compared with the standard signal into a controller (Ballarini and Euler 2003). in Figure 1 (Shih et al. 2005). The servo-control can be modelled at every moment by

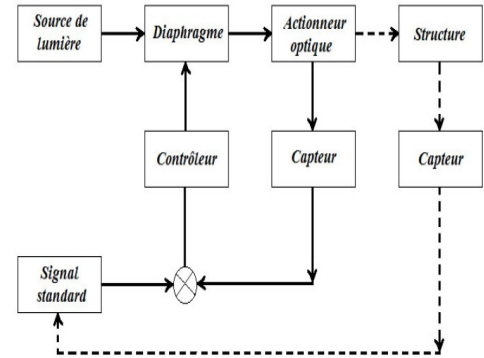


Figure 2 Diagram in block of an optical servo-control (Carlioz 2009).

the following equations:

$$I(t_{j+1}) = G [S_{std}(t_j) - S_{kk}(t_j)], k = 1, 2 \quad (2)$$

$$\theta(t_{j+1}) = \theta(t_j) + \frac{[I(t_{j+1})P - \gamma_0 \theta(t_j)] \Delta t}{H + \gamma_0 \Delta t} \quad (3)$$

$$E_{ph}(t_{j+1}) = [E_s - E_{ph}(t_j)] \alpha_0 I(t_{j+1}) \Delta t e^{-\alpha_0 I(t_{j+1}) \Delta t} - E_{ph}(t_j) \beta_0 \Delta t e^{-\beta_0 \Delta t} + E_{ph}(t_j) \quad (4)$$

$$E_{pyr}(t_{j+1}) = \frac{P}{\epsilon} \theta(t_{j+1}) \quad (5)$$

$$S_{kk}(t_{j+1}) = d_{33} \cdot [E_{ph}(t_{j+1}) + E_{pyr}(t_{j+1})] - \frac{\lambda_3}{Y_a} \theta(t_{j+1}) \quad (6)$$

$S_{std}(t_j)$ Is the standard signal introduced into the servo-control at the moment t_j ; G represents the profit in light intensity of the comparator of the servo, γ_0 rate of $\theta(t_{j+1})$ transferred heat, $\theta(t_{j+1})$ the temperature of the actuator at the moment, t_{j+1} , λ_3 Thermal dilation coefficient, E_{pyr} the pyroelectric electric field, Y_a Young modulus and $k = 1, 2$ the total coordinates.

Mathematical modeling of the beam under control: Let us consider a beam (see Figure 3) length subjected to the action of an axial load P and transversal force q . We suppose that the transverse load $q(x)$ is constant along the element dx and positive if it is directed in the direction of the x axis. The physical and geometrical characteristics of beam are given by Young modulus E , S is the section, I moment of inertia and ρ mass density.

Taking into account the formulation of Nayfeh and Mook (Timoshenko 1966), the general dynamics of the system under control is given by the following equation (7):

$$\rho A \frac{\partial^2 W}{\partial T^2} + \lambda \frac{\partial W}{\partial T} + EI \frac{\partial^4 W}{\partial X^4} + H \left(\frac{\partial^2 W}{\partial X^2} + \frac{\partial^2 W_0}{\partial X^2} \right) + P \frac{\partial^2 W}{\partial X^2} = -Q \quad (7)$$

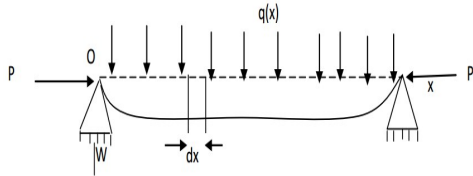


Figure 3 Hinged hinged beam.

The boundary conditions are given by: $W = 0$ et $EI \frac{\partial^2 W}{\partial x^2} = 0$ à $X = 0$ et $X = L$

By introducing the following changes of variables:

$$t = T \frac{\pi^2}{L^2} \sqrt{\frac{EI}{\rho A}}; \quad \omega = \frac{W}{2r}; \quad \omega_0 = \frac{W_0}{2r}; \quad x = \frac{X}{L};$$

$$P = \frac{pL^2}{\pi^2 EI}; \quad q = \frac{QL^4}{2\pi EI r}; \quad \bar{\lambda} = \frac{\lambda}{\sqrt{\rho A EI}}$$

The non-dimensional equation is then given by (Moon 1992), where F is the transversal loads.

$$\begin{aligned} \pi^4 \frac{\partial^2 \omega}{\partial t^2} + \pi^4 C \frac{\partial \omega}{\partial t} + \bar{\lambda} D \frac{\partial^2 \omega}{\partial y^2} + \pi^2 p D \frac{\partial^4 \omega}{\partial x^4} + D \left[\frac{\partial^6 \omega}{\partial x^6} + \frac{\partial^6 \omega}{\partial y^6} \right] &= \frac{\partial^4 M_{yy}^0}{\partial y^4} + \\ \frac{\partial^4 M_{xx}^0}{\partial x^4} + \bar{\lambda} \frac{\partial M_{yy}^0}{\partial y} + \pi^2 p \frac{\partial^2 M_{xx}^0}{\partial x^2} + \pi^4 F & \end{aligned} \quad (8)$$

By applying the method of Galerkin, the vibration of the system to several modes is written in the following form:

$$\omega(x, y, t) = \sum_{n=1}^{\infty} \sum_{m=1}^{\infty} W_{mn}(x, y) \eta_{mn}(t) \sin\left(\frac{m\pi x}{a}\right) \sin\left(\frac{n\pi y}{b}\right) \quad (9)$$

With: $W_{mn} = W_{mn}(x, y) = \sin\left(\frac{m\pi x}{a}\right) \sin\left(\frac{n\pi y}{b}\right)$

The equation of the system becomes then

$$\begin{aligned} \ddot{\eta}_{mn} + \zeta_{mn} \omega_{mn} \dot{\eta}_{mn} + \alpha \omega_{mn}^2 \eta_{mn} + \beta \omega_{mn}^4 \eta_{mn} + \chi \omega_{mn}^6 \eta_{mn} = \\ \frac{1}{\pi^4 N_{mn}} \int_0^a \int_0^b \left[\left(\frac{\partial^4 M_{xx}^0}{\partial x^4} + \frac{\partial^4 M_{yy}^0}{\partial y^4} + \bar{\lambda} \frac{\partial M_{yy}^0}{\partial y} + \pi^2 p \frac{\partial^2 M_{xx}^0}{\partial x^2} \right) \right] \end{aligned}$$

$$\sin\left(\frac{m\pi x}{a}\right) \sin\left(\frac{n\pi y}{b}\right) dx dy = I_{xx} + I_{yy}$$

The equation with the clean modes is then written:

$$\begin{aligned} \ddot{\eta}_{mn} + C \dot{\eta}_{mn} + f_0(t) \delta x * \omega_{mn} \eta_{mn} - \alpha \omega_{mn}^3 \eta_{mn} + \beta \rho \omega_{mn}^4 \eta_{mn} + \\ \chi \omega_{mn}^5 \eta_{mn} - 2m = I_{xx} + I_{yy} = -\tilde{M}_{mnx} - \tilde{M}_{mny} \end{aligned} \quad (10)$$

The differential equation governing the dynamics of the system under control is then obtained.

DYNAMIC RESPONSE OF THE SYSTEM UNDER CONTROL

The force developed by the opto-electromechanical actuator due to illumination and which is at the origin of the deformations S(t) is given by [24] :

$$N_{kk}^0(t_j) = d_{33}^k Y_0 h_0^k \cdot [E_{ph}^k(t_j) + E_{pyr}^k(t_j)] - \lambda_3^k h_0^k \theta^k(t_j) \quad (11)$$

Where the index k = 1, 2 indicates the two plane directions of the total frame of reference. The transverse moment of inflection induced by the plane force $N^0(t_j)$ is:

$$M^0(t_j) = \frac{1}{2} (h + h_0) \cdot \left\{ d_{33} Y_0 h_0 \cdot [E_{ph}(t_j) + E_{pyr}(t_j)] - \lambda_3 h_0 \theta(t_j) \right\} \quad (12)$$

The moments induced according to the total directions (ox) and (oy) are written respectively, considering the local nature of the actuators:

$$M_{xx}^0 = M_{11}^0(t_j) [u_s(x - x_1) - u_s(x - x_2)] \cdot [u_s(y - y_1) - u_s(y - y_2)] \quad (13)$$

$$M_{yy}^0 = M_{22}^0(t_j) [u_s(x - x_3) - u_s(x - x_4)] \cdot [u_s(y - y_3) - u_s(y - y_4)] \quad (14)$$

Maybe, the function of Heaviside defined by:

$$u_s(\chi) = \begin{cases} 1 & \text{if } \chi \geq 0 \\ 0 & \text{if } \chi < 0 \end{cases} \quad (15)$$

After some algebra, one leads to the following differential equations called modal equations:

$$\begin{aligned} \ddot{\eta}_{mn} + \zeta_{mn} \omega_{mn} \dot{\eta}_{mn} + \alpha \omega_{mn}^2 \eta_{mn} + \\ \beta \omega_{mn}^4 \eta_{mn} + \chi \omega_{mn}^6 \eta_{mn} + \tilde{M}_{mnx}^2 + \tilde{M}_{mny}^2 = 0 \end{aligned} \quad (16)$$

While taking into account this equation due to the fact that the actuators are alternatively activated by a servo mechanism according to a given law of control, we now have:

$$\begin{aligned} \ddot{\eta}_{mn} + \zeta_{mn} \omega_{mn} \dot{\eta}_{mn} + \alpha \omega_{mn}^2 \eta_{mn} + \beta \omega_{mn}^4 \eta_{mn} + \\ \chi \omega_{mn}^6 \eta_{mn} + \text{sign}(\dot{\eta}_{mn}) \cdot (\tilde{M}_{mnx}^2 + \tilde{M}_{mny}^2) = 0 \end{aligned} \quad (17)$$

where sign is the function definite by:

$$\text{sign}(x) = \begin{cases} +1 \dots \text{if } \dots x \geq 0 \\ -1 \dots \text{if } \dots x < 0 \end{cases} \quad (18)$$

The equation of the nonlinear system in the presence of the phenomena is thus written as follows:

$$\begin{aligned} \ddot{\eta}_{mn} + C \dot{\eta}_{mn} - \alpha \omega_{mn}^3 \eta_{mn} + \beta \omega_{mn}^4 \eta_{mn} + \chi \omega_{mn}^5 \eta_{mn} - \chi \omega_{mn}^6 \eta_{mn} + \\ \mu x * -2m + \text{sign}(\dot{\eta}_{mn}) \cdot (\tilde{M}_{mnx}^2 + \tilde{M}_{mny}^2) = Q \end{aligned} \quad (19)$$

Where : $Q = f_0 \cos \Omega t$

o f_0 is the amplitude of the external excitation;

o t is time;

o Ω is the frequency of the additive excitation;

$$\begin{aligned} \ddot{\eta}_{mn} + C \dot{\eta}_{mn} + \omega_0^2 \omega_{mn} \eta_{mn} - \alpha \omega_{mn}^3 \eta_{mn} + \gamma \omega_{mn}^4 \eta_{mn} + \chi \omega_{mn}^5 \eta_{mn} - \\ 2m + \text{sign}(\dot{\eta}_{mn}) \cdot (\tilde{M}_{mnx}^2 + \tilde{M}_{mny}^2) = f_0 \cos \Omega t \end{aligned} \quad (20)$$

Let us pose: $\tilde{M}_{mn} = \tilde{M}_{mnx} + \tilde{M}_{mny}$ Where \tilde{M}_{mn} is the moment, the parameter of control which it will be necessary to exploit to optimize control. Thus, we have the equation of the dynamics of a beam under opto-electromechanics control in the form: $\frac{d^2 \eta_{mn}}{dt^2} + C \frac{d\eta_{mn}}{dt} + \omega_0^2 \omega_{mn} \eta_{mn} - \alpha \omega_{mn}^3 \eta_{mn} + \gamma \omega_{mn}^4 \eta_{mn} + \chi \omega_{mn}^5 \eta_{mn} - 2m + \tilde{M}_{mn} \text{sign}(\dot{\eta}_{mn}) = f_0 \cos \Omega t$ Let us pose: $\dot{\eta}_{mn} = \frac{d\eta_{mn}}{dt} = \dot{q} \Rightarrow \eta_{mn} = 1$

with $\omega_{mn} = q$

$$\ddot{\eta}_{mn} + C\dot{\eta}_{mn} + \omega_0^2 \omega_{mn} \eta_{mn} - \alpha \omega_{mn}^3 \eta_{mn} + \gamma \omega_{mn}^4 \eta_{mn} + \chi \omega_{mn}^5 \eta_{mn} - 2m + \tilde{M}_{mn} \text{sign}(\dot{\eta}_{mn}) = f_0 \cos \Omega t \quad (21)$$

$$\ddot{q} + C\dot{q} + \omega_0^2 q - \alpha q^3 + \gamma q^4 + \chi q^5 - 2m + \tilde{M}_{mn} \text{sign}(\dot{q}) = f_0 \cos \Omega t \quad (22)$$

The dynamic behavior of the system is then described by an unlimited ϕ^6 potential whose form is presented below. Thus, beyond a certain amplitude of variation, the limited movements can caused the destruction of the system. The total energy nearest the equilibrium point is given by

$$E = \frac{1}{2}\dot{q}^2 + \frac{1}{2}\omega_0^2 q^2 - \frac{1}{4}\alpha q^4 + \frac{1}{5}\gamma q^5 + \frac{1}{6}\chi q^6 \quad (23)$$

Using the harmonics balance method, one obtains the expression of the force f_0 which is

$$\left(\left(\omega_0^2 - \Omega^2 - \frac{3}{4}\alpha A^2 + \frac{5}{8}\chi A^4 \right) A \right)^2 + \left((c + \text{sign}\tilde{M}_{mn}) A \right)^2 \Omega^2 = f_0^2 \quad (24)$$

with

$$f_0^2 = \frac{25}{64}\chi^2 A^{10} - \frac{15}{32}\alpha\chi A^8 + \left[\frac{5}{4}\chi(\omega_0^2 - \Omega^2) + \frac{9}{16}\alpha^2 \right] A^6 + \left[\frac{3}{2}\alpha(\Omega^2 - \omega_0^2) \right] A^4 + [\omega_0^4 + (c^2 - 2\omega_0^2 + \text{sign}\tilde{M}_{mn})\Omega^2 + \Omega^4] A^2$$

Thus we have the expression of maximum energy given by:

$$E_{\max} = \frac{1}{2}A^2\Omega^2 + \frac{1}{2}(\omega_0^2 - \Omega^2)X_m + \frac{1}{4}\alpha X_m^2 + \frac{1}{6}\chi X_m^3 \quad (25)$$

With: $X_m = \frac{(-\alpha - \sqrt{\alpha^2 - 4\chi(\omega_0^2 - \Omega^2)})}{2\chi}$

Unstable potential energy nearest is as follows:

$$V_c = \frac{1}{2}\omega_0^2 q_c^2 + \frac{1}{4}\alpha q_c^4 + \frac{1}{6}\chi q_c^6 \quad (26)$$

$$X_{m1} = q_1^2 = \frac{-\alpha - \sqrt{\alpha^2 - 4\chi\omega_0^2}}{2\chi} \text{ and } X_{m2} = q_2^2 = \frac{-\alpha + \sqrt{\alpha^2 - 4\chi\omega_0^2}}{2\chi}$$

Consequently, the system and the potential ϕ^6 are stable at the point $q=0$ and unstable at the point q_c . Figure 4 below indicates that the normal position of balance is stable at the point $q=0$ of the structure and that the system can lead to catastrophic motion if the amplitude of vibration become high. Figure 5 shows that the normal position of balance is destabilized and that the dynamics of the system is described by a bistable potential ϕ^6 whose form is presented. The system can either carry out asymmetrical oscillations of low amplitude around one of the two stable positions, or the oscillations of the great amplitude including the two wells. It can also develop unlimited movements including the premature destruction of the structure. Compared to the position, the following equality is checked:

$$E_{\max} = V_c \quad (27)$$

Let us consider the equation (26) with the equation (27), we have:

$$A_b = \left(\frac{2V_c - (\omega_0^2 - \Omega^2)X_m - \frac{1}{2}\alpha X_m^2 - \frac{1}{3}\chi q_m^3}{\Omega^2} \right)^{1/2} \quad (28)$$

Let us insert the equation (28) in the equation (24), we find the amplitude of the excitation.

$$f_0^2 = \left((\omega_0^2 - \Omega^2) A_b - \frac{3}{4}\alpha A_b^3 + \frac{5}{8}\chi A_b^5 \right)^2 + (c\Omega A_b)^2 \quad (29)$$

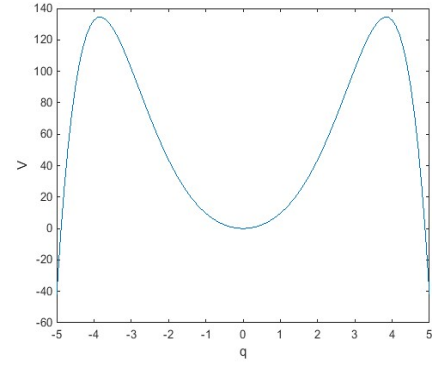


Figure 4 Monostable ϕ^6 potentials

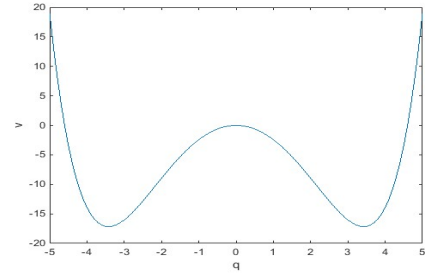


Figure 5 Bistable ϕ^6 potentials

We have also displayed, the variation of the critical force according to the external frequency (Figure 6). We note that the value of critical force $f_c = 0.005$ increases with the external frequency. The amplitude of the minimal critical force is for a frequency $\Omega = 1.5$ which is associated to a primary resonance. Figure 7 displays the

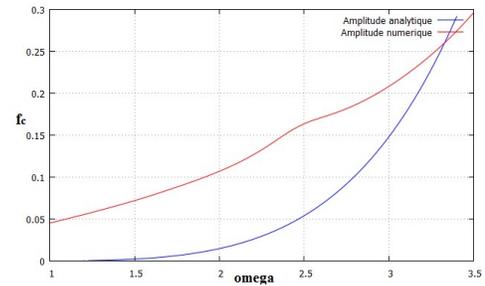


Figure 6 Numerical and analytical amplitude according to the frequency

variation of the critical force according to the parameter of control gain parameter m , it appears that as control parameter decreases, the amplitude of the critical force increases. Consequently, the choice of the parameter of opto-electromechanics control leading to the reduction of the speed and amplitude of vibration tend to control strategy more efficiency.

Figure 8 shows the variation of the critical force according to the moment of actuation, we note that the moment of actuation increases when the variation of the critical force decreases; that shows that control is efficient when the moment of actuation is larger; and is more when the latter becomes increasingly high. A

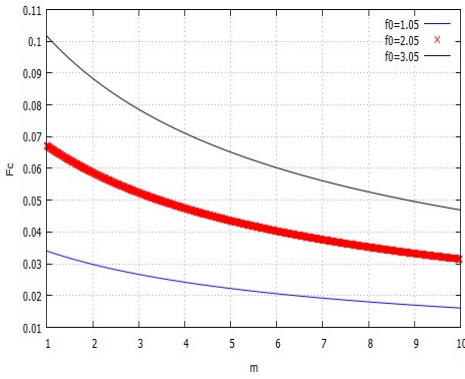


Figure 7 Variation of amplitude of the force criticizes according to the parameter of control m

moment of smaller actuation increases the critical force, that for rather an annoying purpose on the amplitude of vibration of the structure. Figure 9 shows that in the case of variation of the critics

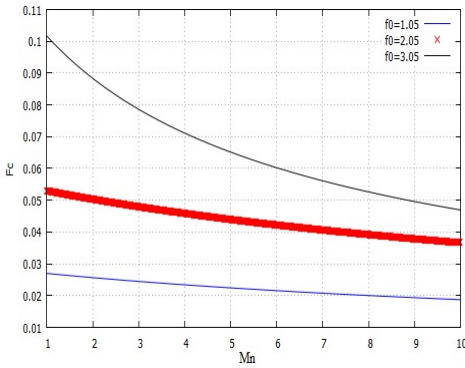


Figure 8 Variation of amplitude of the force criticizes according to the moment of actuation

force leading to the amplification of amplitude, the intensification of amplitude of additive excitation increases the amplitude of the critical force. Otherwise, when the amplitude of additive excitation increases, the variation of the critical force also increases, that tends to delay the possibility of appearance of the chaotic movements.

EFFECT OF OPTO-ELECTROMECHANICAL ACTUATORS ON THE MELNIKOV'S CRITERIA FOR CHAOS

From the Melnikov theory, we derive the analytical criteria for the occurrence of transverse intersections between perturbed and unperturbed separatrix. This brings us to a function which helps to measure the distance between the borders of the regular oscillations and that of the chaotic movements. In this case we focus our attention on the case of unbounded two well potential. Meaning the existence of two Homoclinic and one Heteroclinic orbits. To achieve these goals the first step is to characterise the potential in a space parameter of the system. The potential energy associated the system is given by the relation.

$$V(q) = \frac{1}{2}p^2 + \frac{1}{2}\omega_0^2q^2 - \frac{1}{4}\alpha q^4 + \frac{1}{6}\chi q^6 \quad (30)$$

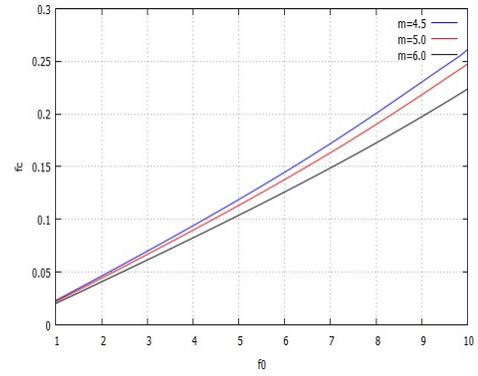


Figure 9 Variation of amplitude of the force criticizes according to amplitude of additive excitation

Equilibrium conditions $\frac{dV(q)}{dq} = 0 \Leftrightarrow \omega_0^2q - \alpha q^3 + \chi q^5 = 0$ five points including three unstable points and two stable points (see Figure 10).

Figure 10 shows that the system can carry out symmetrical oscillations of low amplitude around the point of balance $(0,0)$, asymmetrical oscillations of low amplitude around the degenerated positions of balance, oscillations of great amplitude wrapping the three positions of steady balance. The dynamics of the system is thus described by an unbounded bistable ϕ^6 potential. We

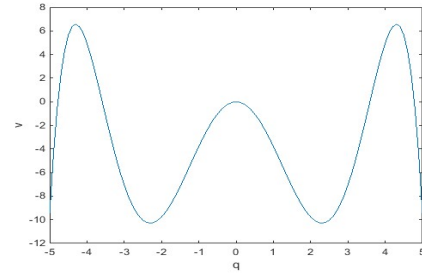


Figure 10 Variations of the potential energy according to electric polarization q

consider a system whose equations of dynamics can be put in the following form:

$$\dot{U} = g_0(U) + \varepsilon g_p(U, t) \quad (31)$$

$\dot{U} = g_0(U) + \varepsilon g_p(U, t)$ Is the vector of state, $g_0 = (g_1, g_2)$ is the field of vector defines by:

$$g_1 = \frac{\partial H_0}{\partial \dot{q}} \text{ and } g_2 = -\frac{\partial H_0}{\partial q} \quad (32)$$

Or H_0 is selected Hamiltonian (non dissipative) of energy and g_0 a periodic function of disturbance such as:

$$g_p(U, t) = (0, -cp + 2m - \tilde{M}_{mn} \text{sign}(p) + f_0 \cos(\Omega\tau)) \quad (33)$$

When there is an intersection between perturbed and unperturbed separatrix, the geometry of the basin of stability can become fractal, indicating the high sensitivity to the initial conditions and carrying chaos. The function of Melnikov is defined by [21-23]:

$$M_e(t_0) = \int_{-\infty}^{+\infty} g_0(\bar{u}(t)) \wedge g_p(\bar{u}(t), t + t_0) \text{ with } -\infty < t < +\infty \quad (34)$$

If $M_e(t_0)$ has of the zero simple ones so that $t_0 \neq 0$, one has $M_e(t_0) = 0$ with $\frac{dH(t_0)}{dt_0} \neq 0$ has $t = t_0$ (the condition for the transverse intersection). To apply the theorem of Melnikov to our model, one must determine the expressions of the homoclinic and heteroclinic orbits of the system. For the case of the Heteroclinic orbit. The Hamiltonian of the system is defined by:

$$H_0(q, \dot{q} = p) = \frac{1}{2}p^2 + \frac{1}{2}\omega_0^2 q^2 - \frac{1}{4}\alpha q^4 + \frac{1}{5}\gamma q^5 + \frac{1}{6}\chi q^6 \quad (35)$$

We obtain the Heteroclinic orbit (connecting the unstable points $-q_c$ and q_c) given by:

$$q = \frac{\pm q_1 \sqrt{2} \sinh((\zeta/2)\tau)}{(-\beta + \cosh(\zeta\tau))^{1/2}}, \quad (36)$$

$$p = \frac{\pm \left(\sqrt{2}/2\right) q_1 (1 - \beta) \zeta \cosh((\zeta/2)\tau)}{(-\beta + \cosh(\zeta\tau))^{3/2}} \quad (37)$$

with $\beta = \frac{(5-3\theta^2)}{(3\theta^2-1)}$, $\zeta = q_1^2 \sqrt{2\chi(\theta^2-1)}$, $\theta = \frac{q_2}{q_1}$ q_1 is the unstable point of balance and q_2 the module of the root of complex equations given by

$$\omega_0^2 - \alpha q^2 + \chi q^4$$

$$q_1^2 = \frac{-\alpha - \sqrt{\alpha^2 - 4\chi\omega_0^2}}{2\chi}, \quad q_2^2 = \frac{\alpha - \sqrt{\alpha^2 - 4\chi\omega_0^2}}{2\chi}$$

And we have the Homoclinic orbit given by the relation:

$$q = \frac{\pm q_1 \sqrt{2} \cosh((\zeta/2)\tau)}{(\beta + \cosh(\zeta\tau))^{1/2}}, \quad p = \frac{\pm \left(\sqrt{2}/2\right) q_1 (\beta - 1) \zeta \sinh((\zeta/2)\tau)}{(\beta + \cosh(\zeta\tau))^{3/2}} \quad (38)$$

With the expressions of the equations (36) - (38), we can proceed and calculate the Melnikov function for each case. In the case of the potential with three wells, calculations lead to the following conditions for the appearance of the chaos of Melnikov are thus: For the case of Heteroclinic separatrix:

$$f_0 \geq f_c = \frac{Cq_1\zeta^2}{8\Omega\pi(\beta+1)} \left[\frac{(2\beta+1)}{(1-\beta^2)^{1/2}} \left(\text{Arc sin } \beta + \frac{\pi}{2} \right) + 2 + \beta \right] \sinh \frac{2\Omega}{\zeta} \quad (39)$$

While for the case of Homoclinic separatrix,

$$f_0 \geq f_c = \frac{Cq_1\zeta^2}{32\Omega\pi(\beta+1)} \left[\frac{(2\beta+1)}{(1-\beta^2)^{1/2}} \left(\text{Arc sin } \beta - \frac{\pi}{2} \right) + 2 + \beta \right] \frac{\zeta}{\sin(2\Omega)} \quad (40)$$

In order to confirm and analyse the effect of controller we display the evolution of critical force as a function of the frequency of response curve. Figure 11 and 12 represent respectively the case of Heteroclinic and Homoclinic separatrix. From these curves, it comes out that the chaotic behavior occurs in the domain above the curve. Considering orbits starting at the points sufficiently close to the separatrix, the criterion of Melnikov is accomplished when the perturbed orbits intersects with the separatrix. These figures also show that the domain for the appearance of horseshoes are opposite taking into account the case of heteroclinic or homoclinic chaos. It appears that as the control gain parameter increases the domain for regular motion also increases. A particular characteristic of the chaos of Melnikov is the fractality of the basin of attraction and the resulting unpredictability due to the dependence with regard to the initial conditions. We have plotted in Figure 13 the basin of attraction in order to confirm or prediction. Setting $\Omega = 0.5$, for various values of parameter of control m , the boundary of the basins are regular thus there are no chaos of Melnikov. We plotted

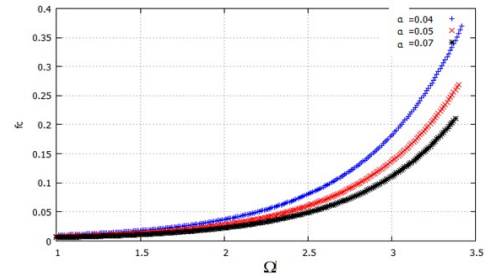


Figure 11 Evolution of critical force as function of to the frequency: case of an Heteroclinic orbit

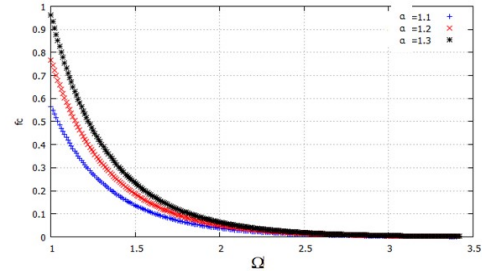


Figure 12 Evolution of critical force as a function of frequency: case of an Homoclinic orbit

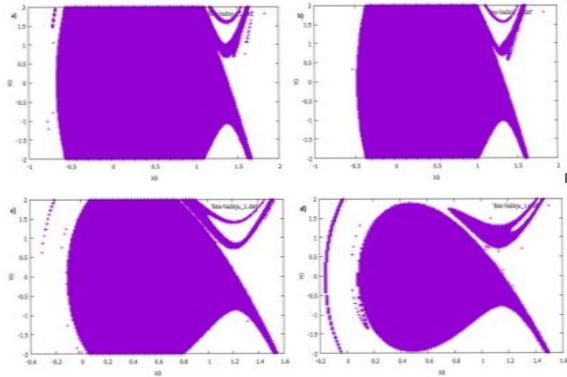


Figure 13 Basin of attraction for $\Omega = 0.5$ a) $m = 0$; b) $m = 1$; c) $m = 3$; d) $m = 4$

in F 14 the basins for $\Omega = 1$, it appears that for various values of control gain parameter m , the boundary of the basin can be regular (see Figure 14 a and 14 b) and become irregular as the control parameter increases (see Figure 14 c and 14 d), meaning that the choice of the control gain parameters has a great influence on the appearance of horseshoes chaos

Concerning the case of $\Omega = 3$ and for certain values of the parameter of control m , the fractality is more visible (see Figure 15). The same observation is done in Figure 16. This means that for the control strategy to be efficient the critical force leading to the appearance of horseshoes is directly related to the value of frequency and control gain parameter.

Consequently, in spite of the fact that the controller reduces speed as well as the amplitude of vibration, it induces the chaos of the horseshoe type in the dynamic behavior of the system. Thus

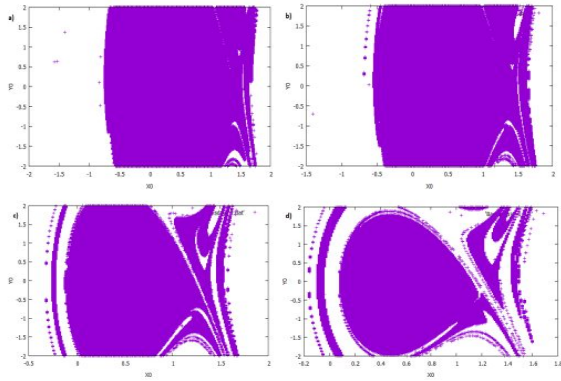


Figure 14 Basin of attraction for $\Omega = 1$ a) $m=0$; b) $m=1$; c) $m=3$; d) $m=4$

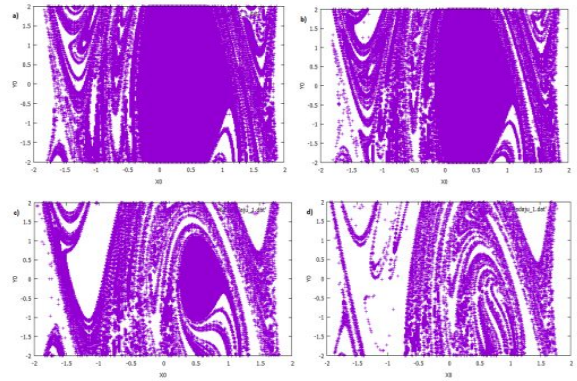


Figure 16 Basin of attraction for $\Omega = 4$ a) $m=0$; b) $m=1$; c) $m=3$; d) $m=4$

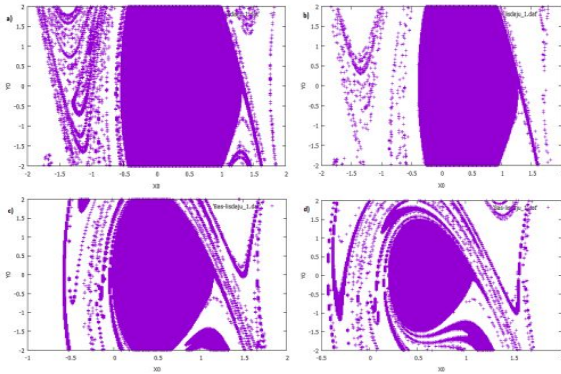


Figure 15 Basin of attraction for $\Omega = 3$ a) $m=0$; b) $m=1$; c) $m=3$; d) $m=4$

the optimization of the strategy of control requires the taking into account of the conditions of appearance of chaos.

CONCLUSION

This paper presented the possibility of reducing the vibration on a structure modelled by Euler beam with ϕ_6 potential using opto-electromechanic actuators. Taking into account the boundary conditions of the physical system and using Galerkin method one leads to the modal equation which is a nonlinear second order ordinary differential equation. The analytical study gives us the possibility to establish the conditions in the space parameters of the system leading to the efficiency of the control. The criteria for the appearance of horseshoe chaos were derived using Melnikov theory. These findings were further supported by numerical simulations of the original nonlinear equation, and transformations in the basin of attraction were observed. The domain in the parameters space of the system leading to homoclinic or heteroclinic transverse intersection has been derived taking into account the value of the control gain parameter of the opto-electromechanic actuators. It appears that, a dissymmetrical distribution of actuators is more effective than a symmetrical distribution for the simple reason that the control region is much more bigger considering the space parameter of the system.

Availability of data and material

Not applicable.

Conflicts of interest

The authors declare that there is no conflict of interest regarding the publication of this paper.

Ethical standard

The authors have no relevant financial or non-financial interests to disclose.

LITERATURE CITED

- Aida, T., K. Kawazoe, and S. Toda, 1995 Vibration control of plates by plate-type dynamic vibration absorbers. *J. Vib. Acoust* **117**: 332–338.
- Ballarini, R. and B. Euler, 2003 Beam theory. Magazine Online, Accessed: [Insert Date].
- Carlioz, L., 2009 *Générateur Piézoélectrique à Déclenchement Thermomagnétique*. Phd thesis, Institut Polytechnique de Grenoble, France.
- Cheng, A., C. Yang, K. Hackl, and M. Chajes, 1993 Stability, bifurcation and chaos of non-linear structures with control ii. non autonomous case. *Int. J. Non-Linear Mech* **28**: 549–565.
- Fukuda, T., S. Hattori, F. Arai, H. Matsuura, T. Hiramatsu, *et al.*, 1993 Characteristics of optical actuator – servomechanisms using bimorph optical piezoelectric actuator. In *Proceedings of 1993 IEEE Robotics and Automation Conference*, pp. 618–623.
- Hackl, K., C. Yang, and A.-D. Cheng, 1993 Stability, bifurcation and chaos of non-linear structures with control i. autonomous case. *Int. J. Non-Linear Mech* **28**: 441–454.
- Liu, B. and H. Tzou, 1998a Distributed photostrictive actuator and opto-piezothermoelasticity applied to vibration control of plates. *Journal of Vibration and Acoustics* **120**: 936–943.
- Liu, B. and H. S. Tzou, 1998b Distributed photostrictive actuation and opto-piezothermoelasticity applied to vibration control of plates. *Journal of Vibration and Acoustics* **120**: 937–943.
- Metsebo, J., B. Abdou, D. T. Ngatcha, I. K. Ngongiah, P. D. K. Kuate, *et al.*, 2024 Analysis of a resistive-capacitive shunted josephson junction with topologically nontrivial barrier coupled to a rlc resonator. *Chaos and Fractals* **1**: 31–37.
- Moon, F., 1992 *Chaotic and Fractal Dynamics*. Wiley, New York.
- Nana Nbandjo, B., R. Tchoukuegno, and P. Woafu, 2003 Active control with delay of vibration and chaos in a double well duffing oscillator. *Chaos, Solitons & Fractals* **18**: 345.
- Nana Nbandjo, B. and P. Woafu, 2007 Active control with delay of horseshoes chaos using piezoelectric absorber on a buckled

- beam under parametric excitation. *Chaos, Solitons & Fractals* **32**: 73.
- Nana Nbandjo, B. R., 2004 *Dynamics and active control with delay of the dynamics of unbounded monostable mechanical structures*. Ph.D. thesis, University of Yaoundé I.
- Ngatcha, D. T., B. P. Ndemanou, A. F. Talla, S. G. N. Mbouna, and S. T. Kingni, 2024 Numerical exploration of a network of nonlocally coupled josephson junction spurred by wien bridge oscillators. *Chaos and Fractals* **1**: 1–5.
- Okada, Y., K. Matsuda, and H. Hashitani, 1995 Self-sensing active vibration control using the moving-coil-type actuator. *J. Vib. Acoust* **117**: 411–415.
- Pinto, O. and P. Goncalves, 2002 Active non-linear control of buckling and vibrations of a flexible buckled beam. *Chaos, Solitons & Fractals* **14**: 227–239.
- Shih, H., H. Tzou, and M. Saypuri, 2005 Structural vibration control using specially configured opto-electromechanical actuators. *Journal of Sound and Vibration* **284**: 361–378.
- Shih, H.-R., 2000 Distributed vibration sensing and control of a piezoelectric laminated curved beam. *Journal of Smart Materials and Structures* **9**: 761–766.
- Shih, H.-R. and H. S. Tzou, 2000 Opto-piezothermoelastic constitutive modeling of a new 2-d photostrictive composite plate actuator. In *Proceedings of ASME IMECE*, volume 61, pp. 1–8.
- Sonfack, H., 2011 *Dynamique et Contrôle par Sandwich des Vibrations d'une Plaque sous Excitation Impulsive Périodique Localisée*. Mémoire de fin d'études, Université de Yaoundé I, Ecole Normale Supérieure, Cameroun, Présenté en vue de l'obtention du grade de Professeur de Lycée d'Enseignement Général.
- Timoshenko, S., 1966 *Théorie de la stabilité élastique*. Imprimerie Jouve, Paris.
- Tzou, H. and C. Chou, 1996 Nonlinear opto-electromechanics and photodeformation of optical actuators. *Journal of Smart Material and Structure* **5**: 230–235.
- Tzou, H. S. and G. L. Anderson, 1992 *Intelligent Structural Systems*. Kluwer Academic Publishers, Boston.
- Uchino, K., 1996 *Piezoelectric Actuators and Ultrasonic Motors*. Kluwer Academic Publishers, Boston.
- Wang, S., S. Quek, and K. Ang, 2001 Vibration control of smart piezoelectric composite plates. *Journal of Smart Materials and Structures* **10**: 637–644.

How to cite this article: Lissan 1er, D. J., Oumarou, S. A., and Nbandjo, B. R. N. Suppression of Catastrophic Motion and Horseshoes Chaos on a Mechanical Structure using Opto-Electromechanicals Devices. *Chaos Theory and Applications*, 7(1), 42-49, 2025.

Licensing Policy: The published articles in CHTA are licensed under a [Creative Commons Attribution-NonCommercial 4.0 International License](https://creativecommons.org/licenses/by-nc/4.0/).

